SiC_2P: A Promising Molecule with Two Stable Cyclic Isomers

Guang-hui Chen,[†,‡] Yi-hong Ding,*[,†] Xu-ri Huang,[†] Hong-xing Zhang,[†] Ze-sheng Li,[†] and Chia-chung Sun[†]

State Key Laboratory of Theoretical and Computational Chemistry, Institute of Theoretical Chemistry, Jilin University, Changchun 130023, People's Republic of China and Department of Chemistry, Mudanjiang Normal University, Mudanjiang 157012, People's Republic of China

Received: May 7, 2002; In Final Form: August 20, 2002

The structures and isomerization of SiC_2P species are explored at various levels. Thirteen minima are located connected by 19 interconversion transition states. At the CCSD(T)/6-311+G(2df)//QCISD/6-311G(d)+ZPVE level, the lowest energy isomer is a linear form SiCCP **1** whose structure mainly resonates between |Si═C═C═P|• and |Si═C•−C≡P| with the former bearing somewhat more weight. The second and third low-lying isomers are cyclic cSiCCP **5** (with Si−C cross-bonding) at just 3.2 kcal/mol and cSiCPC **7** (with C−C cross-bonding) at 10.4 kcal/mol, respectively. All the three isomers **1**, **5**, and **7** possess considerable kinetic stability either toward isomerization or dissociation, and thus are expected to be observable. The calculated results are compared to those of the analogous molecules C_3N, SiC_2N, and C_3P. Implications in the interstellar and P-doped SiC vaporization processes are discussed.

1. Introduction

Silicon and phosphorus chemistry have received considerable attention from various aspects. One particular interest is their possible role in astrophysical chemistry. Up to now, several silicon- or phosphorus-containing molecules, such as SiC_n ($n = 1-4$), SiN, SiO, SiS, PC, and PN, have been detected in interstellar space.[1] Of particular interest, the ground-state structure of SiC_2[2,3] and SiC_3 are cyclic forms.[4] No cyclic species containing phosphorus have been observed in space up to now.

In this work, we study the tetra-atomic molecule SiC_2P, which belongs to the isoelectronic XC_2Y (X = C, Si; Y = N, P) series. Extensive experimental and theoretical investigations[5] have shown that C_3N only have linear CCCN and CCNC with the dominant valence structure •C≡C−C≡N| and •C≡C−N≡C|, respectively. Both C_3N isomers have been detected in interstellar space.[5a] In addition, the analogues C_3P[6] and SiC_2N[7] have received recent theoretical consideration. The ground state of C_3P is linear CCCP (valence structure |C═C═C═P|•) followed by the four-membered ring cC_3P with C−C cross-bonding, while linear CCPC is not a minimum. For SiC_2N, two linear forms SiCCN (valence structure |Si═C•−C≡N|) and SiCNC (valence structure |Si═C•−N≡C|) and a bent SiNCC were predicted to be observable. Several cyclic forms of C_3P and SiC_2N were also located as minima. Clearly, there exist some structural, bonding, and energetic discrepancies between C_3N, C_3P, and SiC_2N. Then it is natural to speculate on the properties of SiC_2P. To our best knowledge, no studies have been reported on SiC_2P. Since many Si-containing molecules have stable cyclic isomers (such as SiC_2, SiC_3, and $Si_2C_2$8), we wonder whether SiC_2P has such stable cyclic forms to allow their laboratory or interstellar identification.

On the other hand, Si- or P-containing species have been believed to play important roles in materials chemistry. Binary silicon carbides are commonly used in microelectronic and photoelectronic applications,[9] while Si−P bonding can be found in various fields such as inorganic, organic, and organometallic chemistry.[10] The knowledge about the structure, energies, and bonding nature of various SiC_2P isomers may be helpful for understanding the initial step of the growing mechanism during the P-doped SiC vaporization process.

2. Computational Methods

Computations are carried out using the GAUSSIAN98[11a] and MOLCAS[11b] (for CASSCF and CASPT2) program packages. The optimized geometries and harmonic vibrational frequencies of the local minima and transition states are obtained at the B3LYP/6-311G(d) theory level. Single-point calculations are performed at the CCSD(T)/6-311G(2d) level using the B3LYP/6-311G(d) optimized geometries. To confirm whether the obtained transition states connect the right isomers, the intrinsic reaction coordinate (IRC) calculations are performed at the B3LYP/6-311G(d) level. The structures, frequencies, and energetics of the relevant species are further calculated at the QCISD/6-311G(d) and CCSD(T)/6-311+G(2df) (energy only) levels. The zero-point vibrational energies (ZPVE) at the 6-311G(d) B3LYP and QCISD levels are also included for energy correction. The multi-reference properties of some structures are checked by additional CASSCF and CASPT2 calculations.

3. Results and Discussions

For conciseness, the results are organized as follows. In Section 3.1, we first present a rough discussion on the stability of SiC_2P isomers. Then for the most relevant species, we give a detailed discussion on the structural and bonding properties in Section 3.2. Where possible, comparisons with the related species are made. In Section 3.3, we assess the possible relevance of SiC_2P in interstellar space and in SiC-vaporization processes. In Section 3.4, a brief assessment of the reliability of methods is given. Unless otherwise specified, the relative energies are at the CCSD(T)/6-311G(2d)//B3LYP/6-311G(d)+ZPVE level (simplified as CCSD(T)//B3LYP).

3.1. SiC_2P PES. The isomeric search follows the scheme: chain [formed from (SiC, CP) and (SiP, C_2) molecule−radical pairs], four-membered ring [from SiCCP and SiCPC rings],

[†] Jilin University.
[‡] Mudanjiang Normal University.

10.1021/jp0211234 CCC: $22.00 © 2002 American Chemical Society
Published on Web 09/28/2002

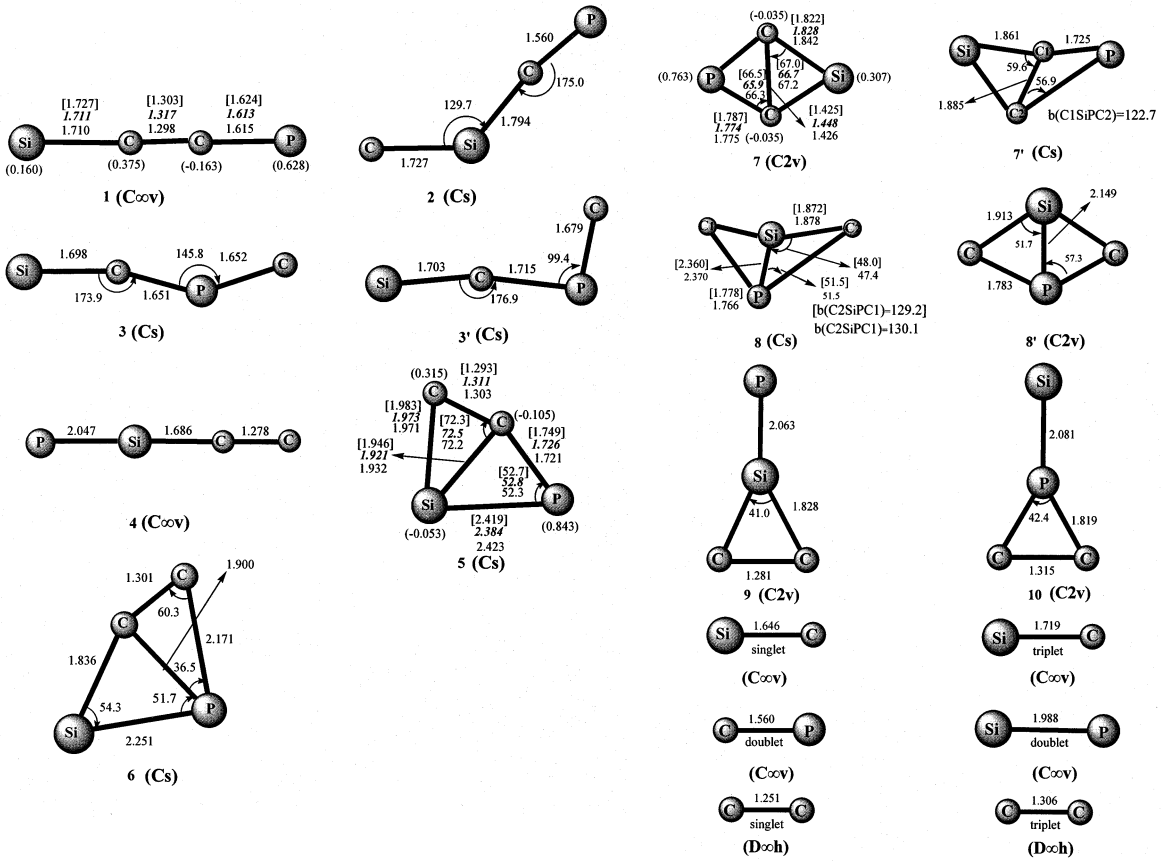

Figure 1. Optimized geometries of SiC_2P various isomers and spin densities (in parentheses) for relevant **1**, **5,** and **7** at the B3LYP/6-311G(d) level. The values in italics are at the QCISD/6-311G(d) level and values in brackets are at the CASSCF(13,13)/6-311G(2df) level. Bond lengths are in angstroms, angles in degrees, and spin density in *e*.

three-membered ring [from the perpendicular-like attack of (SiC, CP) and (SiP, C_2) pairs], and all-closed species. After numerous searches, 13 SiC_2P minimum isomers (**m**) and 19 interconversion transition states (**TSm/n**) are obtained at the B3LYP/6-311G(d) level. The optimized geometries of the SiC_2P isomers and transition states are shown in Figure 1 and Figure 2, respectively. The harmonic vibrational frequencies as well as the infrared intensities, dipole moments, and rotational constants of the SiC_2P species are listed in Table 1, while the total and relative energies of all species are collected in Table 2. A schematic potential-energy surface (PES) of SiC_2P is presented in Figure 3.

On the PES, the lowest-lying isomer is linear SiCCP **1** (0.0). The other linear or bent species CSiCP **2** (71.7), SiCPC **3** (84.4), SiCPC **3′** (87.6), and PSiCC **4** (51.8) with internal −Si−X− or −P−X− bonding are energetically very high. No CSiPC form can be located as a minimum. SiPCC is not a minimum, either, although the analogous SiNCC has been predicted as an important minimum on the SiC_2N PES.[7] The second, third, and fourth low-lying isomers are all planar four-membered ring species, i.e., cSiCCP **5** (6.8) with Si−C cross-bonding, cSiCPC **7** (14.1) with C−C cross-bonding, and cSiCCP **6** (22.8) with P−C cross-bonding. Note that **7** has a high-energy isomer **7′** (43.7) with a butterfly-like structure. The use of CCSD(T)/6-311+G(2df)//QCISD/6-311G(d)+ZPVE single-point calculations (simplified as CCSD(T)//QCISD) even lower the relative energies of the species **5** and **7** to be 3.2 and 10.4 kcal/mol, respectively. The species **8** (72.9) (butterfly-like) and **8′** (80.4) (planar) both possess SiCCP four-membered ring structures with Si−P cross-bonding. It is worthwhile to point out that **7′** actually correlates with the $^2A_2$ state and **8** with the $^2B_1$ state. The respective planar $^2A_2$ and $^2B_1$ structures each possess one out-of-plane imaginary frequency and lie 4.3 and 7.0 kcal/mol above **7′** and **8**, respectively. The remaining two isomers P−cSiCC **9** (45.6) and Si−cPCC **10** (70.3) are both three-membered ring structures. At the HF level, the three-membered ring species C−cCSiP and P−cCSiC are local minima, yet each collapses to the four-membered ring species **5** at the B3LYP level. Optimization of Si−cCCP, C−cSiCP, and C−cPSiC usually leads to the chainlike species **1**, **2**, **3**, or **3′**. The closed tetrahedral-like structures cannot be located as minima, either.

To discuss the kinetic stability, one needs to consider various isomerization and dissociation pathways as many as possible. Since the relative energies of the dissociation products Si+CCP, P+CCSi, SiP+C_2, and SiC+CP are rather high (more than 100 kcal/mol at the CCSD(T)//B3LYP level) as shown in Table 2, we did not attempt to search any dissociation transition states. So the isomerization process governs the kinetic stability of SiC_2P isomers. For simplicity, the details of the obtained 19 transition states are omitted. We can see that only the three isomers **1**, **5**, and **7** may be of interest with considerable kinetic stability. The linear isomer **1** and the cyclic one **7** has comparable kinetic stability as 21.3 (*20.8*) and 24.4 (*25.6*) kcal/mol, and the cyclic **5** has a slightly lower kinetic stability 14.5 (*17.6*) kcal/mol. The italic values in parentheses are for CCSD(T)//QCISD single-point calculations. Under low-temperature conditions (such as in dense interstellar clouds), such kinetic stability is high enough to allow the existence of the three species. At very high temperature, **5** may isomerize to **1** with the barrier 14.5 (*17.6*) kcal/mol. Yet, the **7** → **1** conversion is much more difficult since the easiest pathway has to encounter two low-lying intermediates **6** and **5** with two considerable

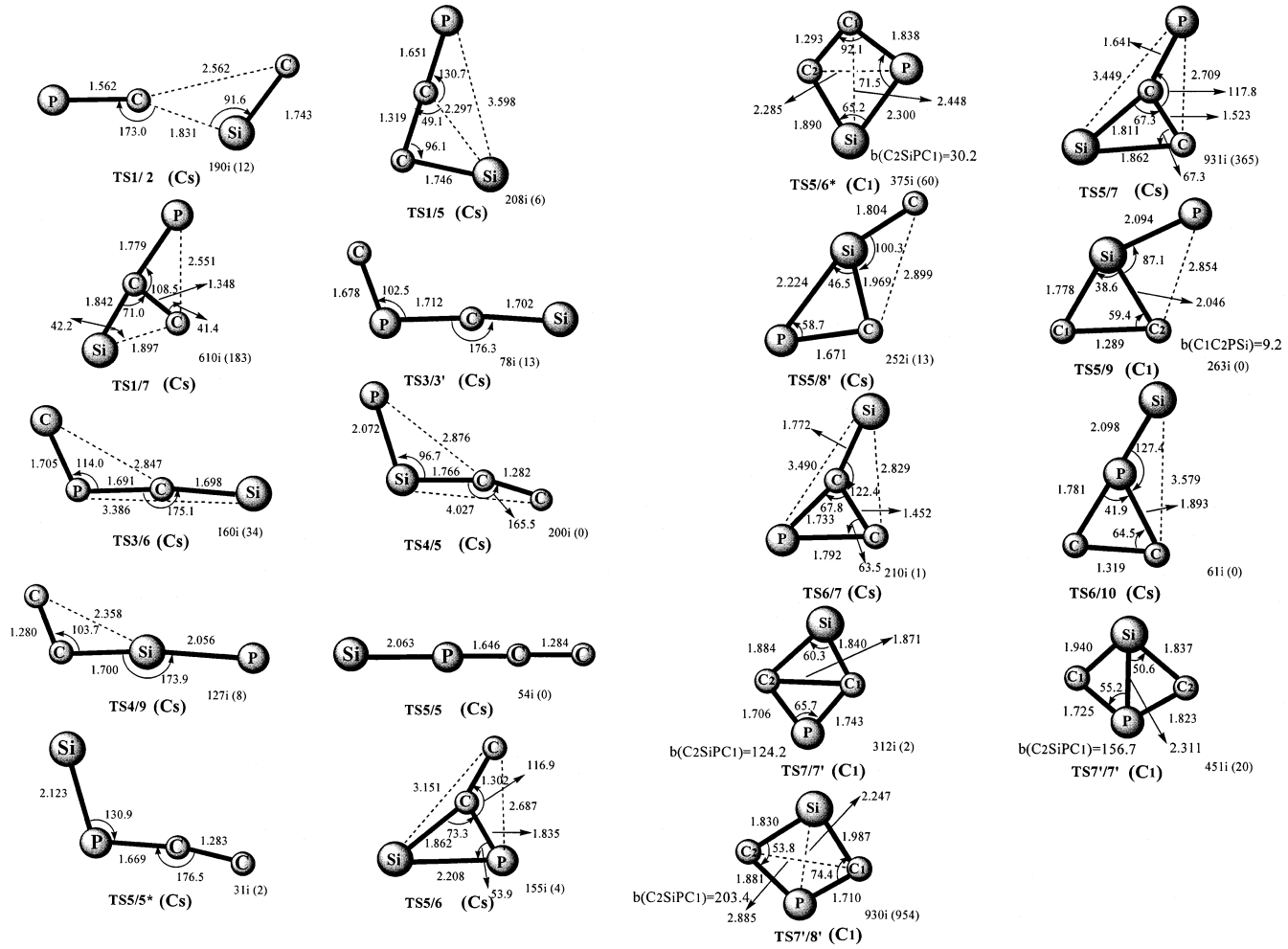

Figure 2. Optimized geometries and imaginary frequencies of SiC_2P transition states at the B3LYP/6-311G(d) level. Bond lengths are in angstroms and angles in degrees.

TABLE 1: Harmonic Vibrational Frequencies (cm^{-1}), Infrared Intensities (km/mol) (in parentheses), Dipole Moment (Debye), and Rotational Constants (GHZ) of SiC_2P Structures at the B3LYP/6-311G(d) Level[b]

species	frequencies (infrared intensity)	dipole moment	rotational constant
SiCCP **1**	127 (2) 144 (6) 391 (0) 460 (1) 518 (16) 1064 (0) 1738 (343)	1.1088	1.558034
SiCCP **1**[a]	116 (2) 136 (7) 342 (0) 404 (1) 517 (12) 1070 (0) 1652 (384)	0.8398	1.544677
CSiCP **2**	97 (14) 226 (8) 238 (18) 501 (18) 920 (3) 1427 (0)		
SiCPC **3**	88 (5) 169 (11) 177 (13) 512 (11) 1017 (63) 1328 (122)		
SiCPC **3′**	56 (10) 199 (11) 205 (21) 497 (8) 972 (27) 1247 (44)		
PSiCC **4**	69 (9) 89 (6) 147 (10) 175 (6) 486 (2) 846 (6) 1931 (741)		
cSiCCP **5**	223 (11) 318 (6) 499 (11) 655 (51) 758 (17) 1595 (3)	2.5950	11.64189, 4.85468, 3.42602
cSiCCP **5**[a]	266 (11) 317 (6) 514 (11) 668 (41) 781 (22) 1596 (1)	2.7836	11.66597, 4.93925, 3.47006
cSiCCP **6**	205 (3) 245 (1) 361 (9) 524 (17) 703 (26) 1676 (78)		
cSiCPC **7**	252 (7) 352 (50) 511(21) 862 (0) 936 (7) 1161 (6)	0.0889	41.42706, 3.11281, 2.89527
cSiCPC **7**[a]	258 (8) 372 (50) 535 (20) 880 (0) 974 (9) 1143 (17)	0.1386	40.15051, 3.15967, 2.92915
cSiCPC **7′**	231 (4) 323 (9) 414 (17) 529 (31) 767 (59) 994 (54)		
cSiCPC **8**	372 (17) 432 (6) 509 (1) 646 (0) 692 (1) 804 (1)		
cSiCPC **8′**	241 (91) 307 (1) 478 (6) 619 (7) 627 (4) 762 (0)		
P−cSiCC **9**	151 (14) 155 (18) 381 (30) 482 (3) 862 (149) 1772 (5)		
Si−cPCC **10**	43 (0) 68 (1) 353 (33) 475 (40) 745 (15) 1524 (0)		

[a] At the QCISD/6-311G(d) level. [b] For the relevant isomers, the QCISD/6-311G(d) values are included also.

barriers 24.4 (*25.6*) (**7** → **6**) and 14.5 (**5** → **1**) kcal/mol (the conversion from **6** to **5** is easy with the barrier 3.1 kcal/mol). The direct isomerization barrier from **7** to **1** is even much higher as 36.1 kcal/mol.

However, apart from **1**, **5**, and **7**, the other isomers have much lower kinetic stability. At the CCSD(T)//B3LYP level, the least isomerization barriers of the species **2**, **3**, **3′**, **4**, **6**, **7′**, **8′**, **9**, and **10** are 3.9 (**2** → **1**), 3.2 (**3** → **3′**), 0.0 (**3′** → **3**), −2.1 (**4** → **9**), 3.1 (**6** → **5**), −0.1 (**7′** → **7**), 3.8 (**8′** → **7′**), 4.1 (**9** → **4**), and 0.7 (**10** → **6**) kcal/mol, respectively. Coupled with their high energy, they may be of little interest as observable species either in the laboratory or in space. Interestingly, although the **7′** → **7** conversion is not allowed under the C_s-symmetry since **7′** and **7** correlate with different states, it can proceed barrierlessly via an intersystem-crossing **TS7/7′** with C_1-symmetry. Yet, a similar search of **TS8/8′** is unsuccessful. In fact, we cannot locate any

TABLE 2: Relative Energies (kcal/mol) of the SiC_2P Structures and Transition States at the B3LYP/6-311G(d) and Single-Point CCSD(T)/6-311G(2d) Levels[f]

species	B3LYP[b]	ΔZPVE B3LYP[b]	CCSD(T)[c] //B3LYP[b]	total 1	QCISD[b]	CCSD(T)[d] //QCISD[b]	ΔZPVE QCISD[b]	total 2	CASPT2//CASSCF[e](13,13)
SiCCP **1** ($^2\Pi$)[a]	0.0	0.0	0.0	0.0	0.0	0.0	0.0	0.0	0.0
CSiCP **2** (^{2}A′)	84.2	−1.5	73.2	71.7					
SiCPC **3** (^{2}A′)	90.8	−1.6	86.0	84.4					
SiCPC **3′** (^{2}A′)	94.0	−1.8	89.4	87.6					
PSiCC **4** ($^2\Pi$)	55.2	−1.0	52.8	51.8					
cSiPCC **5** (^{2}A″)	14.0	−0.6	7.4	6.8	8.5	3.3	−0.1	3.2	5.3
cSiPCC **6** (^{2}A″)	30.0	−1.0	23.8	22.8					
cCSiCP **7** ($^2B_1$)	18.8	−0.5	14.6	14.1	10.8	10.5	−0.1	10.4	12.6
cCSiCP**7′** (^{2}A″)	54.3	−1.7	45.4	43.7					
cCSiCP **8** (^{2}A′)	88.0	−1.4	74.3	72.9					
cCSiCP **8′**($^2A_2$)	93.6	−2.0	82.4	80.4					
P-cSiCC **9** ($^2B_1$)	52.6	−1.0	46.6	45.6					
Si-cPCC **10** ($^2B_1$)	77.6	−1.8	72.1	70.3					
Si^3 + PCC($^2\Pi$)	114.0	−2.0	107.3	105.3					
P^2 + SiCC($^1\Sigma$)	126.8	−2.3	116.9	114.6					
SiC($^1\Sigma$)+CP($^2\Sigma$)	186.3	−3.0	163.4	160.4					
SiC($^3\Pi$)+CP($^2\Sigma$)	159.6	−3.1	148.2	145.1					
SiP($^2\Sigma$)+C_2($^1\Sigma$g)	180.5	−2.7	144.8	142.1					
SiP($^2\Sigma$)+C_2($^3\Pi$u)	157.8	−2.9	147.2	144.3					
TS1/2 (^{2}A′)	86.7	−1.8	77.4	75.6					
TS1/5 (^{2}A″)	23.4	−0.7	22.0	21.3	22.9	21.2	−0.4	20.8	
TS1/7 (^{2}A″)	54.9	−1.7	51.9	50.2					
TS3/3′ (^{2}A′)	93.9	−1.9	89.5	87.6					
TS3/6 (^{2}A″)	93.4	−2.1	91.3	89.2					
TS4/5 (^{2}A′)	76.0	−1.6	74.9	73.3					
TS4/9 (^{2}A′)	57.3	−1.2	50.9	49.7					
TS5/5(^{2}A′)	64.8	−1.5	62.8	61.3					
TS5/5*(^{2}A″)	64.6	−1.5	64.6	63.1					
TS5/6 (^{2}A″)	31.9	−1.3	27.2	25.9					
TS5/6*	39.6	−1.3	33.6	32.3					
TS5/7(^{2}A″)	62.8	−0.7	58.2	57.5					
TS5/8′ (^{2}A″)	118.8	−2.6	112.4	109.8					
TS5/9	72.9	−1.6	68.3	66.7					
TS6/7 (^{2}A″)	43.2	−1.4	39.9	38.5	37.0	37.0	−1.0	36.0	
TS6/10(^{2}A″)	77.9	−1.8	72.8	71.0					
TS7/7′	54.3	−2.0	45.6	43.6					
TS7′/7′	99.5	−2.0	89.4	87.4					
TS7′/8′	97.5	−2.5	86.7	84.2					

[a] The total energies of reference isomer **1** at the B3LYP/6-311G(d) level are −706.9874776 au, at CCSD(T)/6-311G(2d)// B3LYP/6-311G(d) level is −705.8166099 au, at the QCISD/6-311G(d) level is −705.7516064 au, and at the CCSD(T)/6-311+G(2df)//QCISD/6-311G(d) level is −705.8738824 au, at the CASPT2//CASSCF(13,13) level is −706.1451397006 au. The ZPVE at B3LYP and QCISD level are 0.010111 and 0.009655 au, respectively. [b] The basis set is 6-311G(d) for B3LYP and QCISD. [c] The basis set is 6-311G(2d) for CCSD(T). [d] The basis set is 6-311+G(2df) for CCSD(T). [e] The 6-311G(2df) basis set and 13*13 electrons and active orbitals are used for the CASSCF and CASPT2 method. [f] For the relevant isomers, the CCSD(T)/6-311+G(2df)//QCISD/6-311G(d) and CASPT2(13,13)/6-311G(2df)//CASSCF(13,13)/6-311G(2df) values are included also. The symbols in parentheses of the column denote the point group symmetry.

transition states of **8**. Fortunately, **8** is very high-lying (72.9 kcal/mol above **1**). We expect it to be of little importance in the investigation of SiC_2P isomerization.

3.2. Properties of SiCCP 1, cSiCCP 5, and cSiCPC 7. In Section 3.1, we know that only the three isomers SiCCP **1**, cSiCCP **5,** and cSiCPC **7** possess considerable kinetic stability and may be observable in the laboratory and in interstellar space. We now analyze their structural and bonding properties at the B3LYP/6-311G(d) level. For parallel comparison on the Si−P, C−P, C═P, C−C, C═C, C≡C, Si−C, Si═C, and Si≡C bonding, additional B3LYP/6-311G(d,p) or B3LYP/6-311G(d) calculations (with frequency confirmation as stationary points) are carried out for the structures of model systems SiH_3PH_2, CH_3PH_2, CH_2PH, CH_3CH_3, C_2H_4, C_2H_2, C_6H_6, SiH_3CH_3, $SiCH_2$, HSiCH, CCCN ($^2\Sigma$, $^2\Pi$), and CCCP ($^2\Sigma$, $^2\Pi$). In the following, the bond length comparisons are made with the above B3LYP/6-311G(d,p) results.

The ground state of the lowest-energy isomer SiCCP **1** has the $^2\Pi$ electronic state. Its calculated SiC bond length (1.710 Å) is very close to that (1.713 Å) of the typical Si═C double bonding in $Si{=}CH_2$. Its CP bond value (1.615 Å) lies well between the normal C≡P (1.560 Å) and C═P (1.673 Å) bond lengths. Then, isomer **1** may be best described as a resonant structure between |Si═C═C═P|• and |Si═C•−C≡P|. The calculated Mülliken spin density (0.160, 0.375, −0.163, and 0.628*e* for Si, C, C, and P) indicates that the former structure bears somewhat more weight. The smaller spin density on the terminal silicon shows a very slight contribution from the form •Si≡C−C≡P|. The symbols "•" and "|" denote the single electron and lone-pair electrons, respectively. The above structural description is also supported by the natural bond orbital (NBO) analysis. In fact, the internal CC bond length (1.298 Å) of SiCCP **1** is significantly shorter than that (1.369 Å) of CCCN (described as •C≡C−C≡N| with $^2\Sigma$ state). Yet, the bond lengths of SiC (1.710 Å), CC (1.298 Å), and CP (1.615 Å) in SiCCP **1** are relatively closer to those (1.700 and 1.342 Å for SiC and CC) in SiCCN (dominant structure |Si═C•−C≡N| with $^2\Pi$ state)[7] and (1.309 and 1.596 Å for CC and CP) in CCCP (dominant structure |C═C═C═P•| with $^2\Pi$ state). It seems that the bonding type of SiCCP **1** is right between SiCCN and CCCP with the latter being more akin. Our calculated result that CSiCP **2**, SiCPC **3** and **3′** are energetically much higher

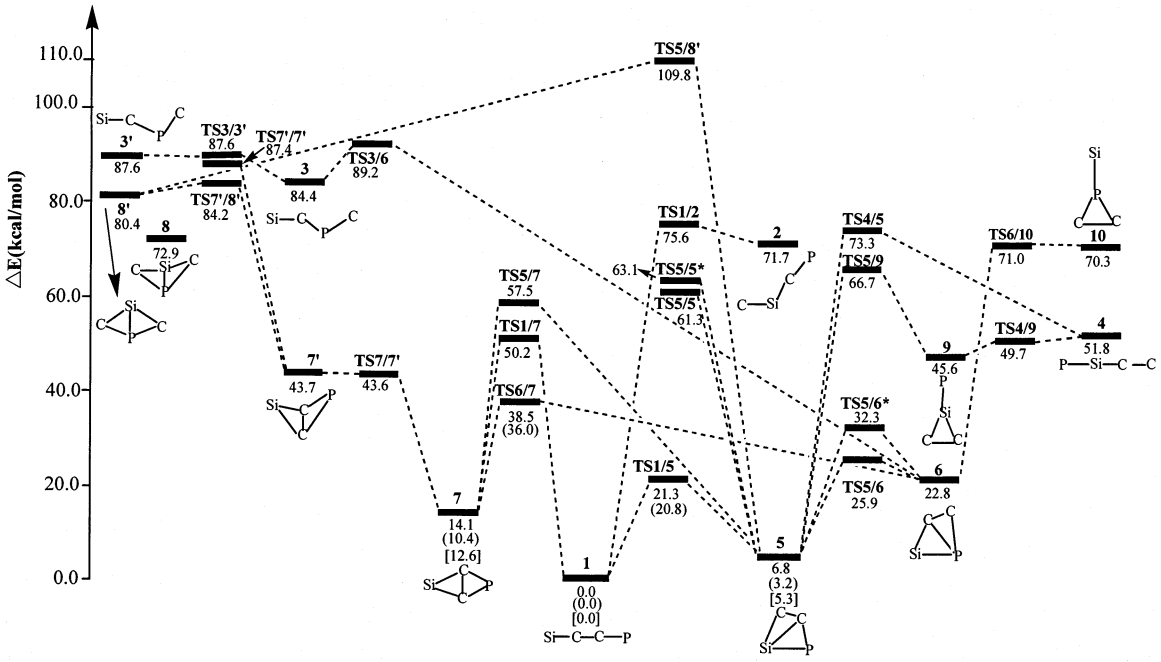

Figure 3. Schematic potential-energy surface of SiC_2P at the CCSD(T)/6-311G(2d)//B3LYP/6-311G(d)+ZPVE level. The relative values in parentheses are at the CCSD(T)/6-311+G(2df)//QCISD/6-311G(d)+ZPVE level, and those in brackets are at the CASPT2/6-311G(2df)//CASSCF/6-311G(2df) level.

TABLE 3: Bond Lengths (in Å) of the $^2\Sigma$ and $^2\Pi$ Structures of the XCCY (X = C, Si; Y = N, P) Species as Well as the Energy Difference (in kcal/mol) between the Two States at the B3LYP/6-311G(d) Level

	$^2\Sigma$			$^2\Pi$			ΔE
(X, Y)	R(XC)	R(CC)	R(CY)	R(XC)	R(CC)	R(CY)	($^2\Pi - {}^2\Sigma$)
(C, N)	1.207	1.369	1.158	1.291	1.341	1.173	0.3
(C, P)	1.217	1.357	1.556	1.292	1.309	1.596	−12.1
(Si, N)				1.700	1.342	1.178	−35.3
(Si, P)				1.710	1.298	1.615	−48.0

TABLE 4: Spin Density of the $^2\Sigma$ and $^2\Pi$ Structures of the XCCY (X = C, Si; Y = N, P) Species at the B3LYP/6-311G(d) Level

	$^2\Sigma$				$^2\Pi$			
(X, Y)	X	C	C	Y	X	C	C	Y
(C, N)	1.210	−0.186	0.074	−0.098	0.289	0.499	−0.139	0.352
(C, P)	1.261	−0.194	0.167	−0.234	0.271	0.292	−0.097	0.533
(Si, N)					0.173	0.627	−0.173	0.373
(Si, P)					0.160	0.375	−0.163	0.628

than SiCCP **1** is surely consistent with the fact that the −Si═C and −P═C units are much less stable than the corresponding −C═Si and −C≡P units. Isomer **1** possesses the "best" combination of −C═Si and −C≡P units.

It is of interest to compare the energetics of the $^2\Sigma$ and $^2\Pi$ electronic states of SiCCP. Similar to the situation of SiC_2N, the $^2\Sigma$ state structure **1′** with the valence form •Si≡C−C≡P| (indicated by spin density and NBO analysis) can only be located at the ab initio levels (HF, MP2, and QCISD). At the B3LYP level, optimization of **1′** always leads to isomer **1** with $^2\prod$ state. The failure may be ascribed to the fact that the HOMO-LUMO gap at the B3LYP level is usually very small compared to the ab initio levels. As a result, the σ HOMO orbital of the $^2\Sigma$ state is easily switched to the π LUMO orbital of the much lower-energy $^2\Pi$ state. Tables 3 and 4 summarize the bond lengths, the $^2\Pi-{}^2\Sigma$ energy gap, and spin density of XCCY (X = C, Si; Y = N, P) species. We can find that along the sequence (C, N), (C, P), (Si, N), and (Si, P), the $^2\Pi-{}^2\Sigma$ energy gap is significantly increased, suggestive of the much decreased X≡C contribution over X═C.

Isomer cSiCCP **5** has a crossed SiC bond (1.932 Å), which is about 0.05 Å longer than the typical Si−C single bond (1.885 Å) in SiH_3CH_3. The peripheral SiC (1.971 Å) and SiP (2.423 Å) bond values are slightly longer than the typical Si−C single bond and Si−P single bond (2.282 Å in SiH_3PH_2), respectively. The peripheral PC bond (1.721 Å) is between the normal P−C single bond (1.872 Å) in CH_3PH_2 and P═C double bond (1.670 Å) in CH_2PH. The peripheral CC bond length (1.303 Å) lies between the calculated typical C═C double bond (1.327 Å) in ethylene (C_2H_4) and the C≡C triple bond (1.198 Å) in acetylene (C_2H_2). The distribution of the spin density is 0.843, −0.053, 0.315, and −0.105*e* for P, Si, C, and C, respectively, along the clockwise ordering as shown in Figure 1. Therefore, isomer **5** can be viewed as associated with the following three resonance structures:

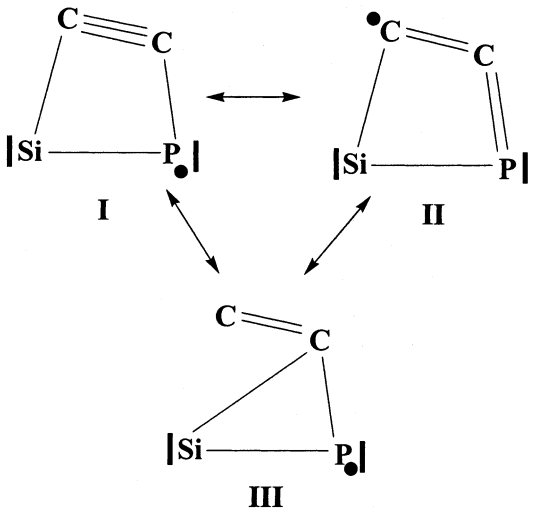

The symbols "•" and "|" denote the single electron and lone-pair electrons, respectively. Structure **I** may contribute the most

TABLE 5: Bond Lengths (in Å) of the C_s-Structure of XCCY Species as Well as the Energy (in kcal/mol) Relative to the Ground State Linear Structures at the B3LYP/6-311G(d) Level

	peripheral bond		cross bond	relative	kinetic
(X, Y)	R(SiC)	R(CC)	R(SiC)	energy	stability
(Si, C)	2.034	1.349	1.888	13.1	
(Si, N)	1.971	1.344	1.879	33.7	0.8
(Si, P)	1.971	1.303	1.932	14.0	17.6
(Si, Si)	1.992	1.313	1.946	8.2	

and **III** the least. The above resonance description is consistent with the NBO analysis.

Isomer **7** is a C_{2v}-symmetrized planar structure with two sets of identical peripheral bonds (i.e., SiC and CP). The SiC bond (1.842 Å) is very close to the typical Si−C single bond (1.885 Å) in SiH_3CH_3. Yet, the CP (1.775 Å) bond is right between the normal single (1.872 Å in CH_3PH_2) and double (1.670 Å in CH_2PH) bonds. Interestingly, the bridged CC bonding is very strong with the bond value 1.426 Å, which lies right between the normal C═C double bond (1.327 Å in ethylene C_2H_4) and C−C single bond (1.530 Å in ethane C_2H_6). This indicates that the crossed CC bond in isomer **7** contains significant double-bonding character, which is quite different from the lower-lying isomer **5** that has a relatively weaker Si−C cross bonding (about 0.05 Å longer than the normal single bond). In fact, the crossed CC bond length is very close to the six identical CC bond value (1.394 Å) in benzene (C_6H_6). Within isomer **7**, the spin density is mainly on the P atom (0.763*e*) with a small part on the Si-atom (0.307*e*), almost zero on the two C-atoms (−0.035*e* for each). Then, isomer **7** can be described as the following resonance picture:

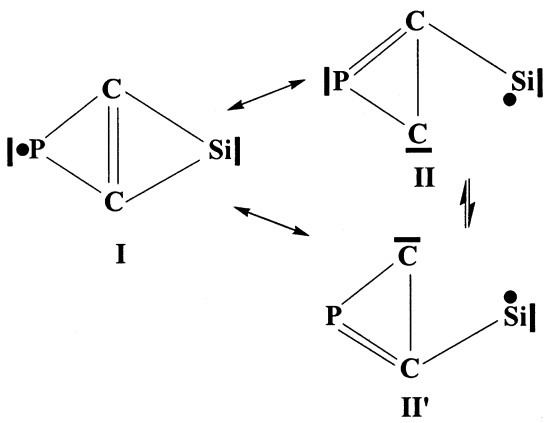

Form **I** has the most weight, followed by **II** and **II′** that have equal contribution. For a simplified form, it can be depicted as:

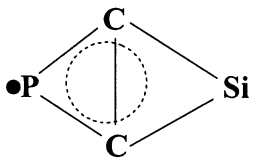

The dashed cycle shows that the electron density mainly delocalizes along the PCC three-membered ring, making PC and CC strong partial double bonding, whereas little resides on the SiCC ring, making SiC merely single bonding.

It is helpful to compare the structural properties of isomers **5** and **7** with the related cyclic species such as SiC_3, Si_2C_2, C_3P, and SiC_2N, as shown in Tables 5 and 6. Here, C_3N is not included since its cyclic forms have not been reported in the literatures and are expected to be of minute importance in view of the high preference of nitrogen to form multiple bonding. To make the following discussion easier, a structure like **5** is called the "C_s-structure", while that like **7** as the "C_{2v}-structure". Concerning the peripheral SiC and CC as well as the cross SiC bond lengths of the C_s-structure, SiC_2P seems to be more akin to Si_2C_2 than to SiC_2N and SiC_3 (despite the spin multiplicity difference). This may be understandable since the electronegativity of phosphorus is more neighboring to silicon than to carbon and nitrogen. The electronegativity difference between Si and Y elements may influence the extent of the electron delocalization within the SiCCY ring. For the C_{2v}-structure, the peripheral SiC and crossed CC bonds of SiC_2P are rather closer to Si_2C_2 than to the other species. In all, although the kinetic stability of C_3N and C_3P has not been reported, we may still expect that along the sequence C_3N, SiC_2N, C_3P, and SiC_2P the cyclic species may become increasingly important relative to the linear form. Both the thermodynamic and kinetic stabilities of the cyclic forms may be increased.

TABLE 6: Bond Lengths (in Å) of the C_{2v}-structure of XCCY Species as Well as the Energy (in kcal/mol) Relative to the Ground-State Linear Structures at the B3LYP/6-311G(d) Level

	peripheral bond	cross bond	relative	kinetic
(X, Y)	R(SiC)/[R(CP)]	R(CC)	energy	stability
(Si, C)	1.837	1.484	8.2	
(Si, N)	1.881	1.479	42.7	5.9
(Si, P)	1.842 [1.775]	1.426	18.8	25.6
(Si, Si)	1.840	1.430	1.4	
(C, P)	[1.776]	1.474	29.1	

3.3. Interstellar and Laboratory Implications. Since the three SiC_2P forms **1**, **5,** and **7** are all predicted to have very low-lying energies accompanied by considerable kinetic stability, they may be observable in both the laboratory and in interstellar space. Up to now, several silicon- or phosphorus-containing molecules, such as SiC_n ($n = 1-4$), SiN, SiO, SiS, PC, and PN, have been detected in space. Among these, cyclic SiC_2 and SiC_3 forms have also been detected. However, observation of the phosphorus-containing species has not been reported. In view of the energies, the direct addition between the atomic ^{3}Si and CCP radical, atomic ^{2}P and CCSi molecule, and the SiC molecule and CP radical may possibly lead to the linear form SiCCP **1**. The cyclic forms **5** and **7** may be generated via effective ion−molecule reactions. Alternatively, the P atom of the doublet SiP radical perpendicularly may attack the CC multiple bonding of either singlet or triplet C_2 to form the three-membered ring isomer **10**. Then **10** can almost barrierlessly lead to isomer **5**, **1,** and even **7** via the intermediate **6**.

It should be pointed out that in the laboratory, both the cyclic (the C_s- and C_{2v}-structures) Si_2C_2 forms have been observed in the Si_n and C_n co-vaporization processes. In view of the many structural similarities existing between the cyclic forms of SiC_2P and Si_2C_2, we hope that the two cyclic SiC_2P forms **5** and **7** and even the linear form may also be detected in P-doped SiC-vaporization processes. The present theoretical paper is expected to stimulate future interstellar and laboratory detection of the Si, P-containing species **1**, **5,** and **7**.

On the other hand, the present calculations on SiC_2P may be related to the microelectronic and photoelectronic technologies. Phosphorus is usually used as a minute dopant. During the P-doped SiC vaporization process, the smaller tetra-atomic species SiC_2P may be generated. Then, the calculated properties and isomerization of various SiC_2P isomers may be helpful for understanding the initial step of the growing mechanism.

To aid in future experimental and interstellar characterization, the QCISD/6-311G(d) harmonic vibrational frequencies, dipole moments, and rotational constants are collected for the three species **1**, **5,** and **7** in Table 1. The dominant vibrational band for **1**, **5,** and **7** is 1652, 668, and 372 cm^{-1}, respectively, with the corresponding infrared intensity 384, 41, and 50 km/mol. In addition, isomer **5** has a large dipole moment 2.7836 D, making it very promising for microwave detection.

3.4. Reliability of the Methods. We performed CASPT2//CASSCF calculations to check the reliability of the present monoconfigurational-based methods (B3LYP, QCISD, and CCSD)—considering 13 frontier orbitals as active space and 13 electrons were allowed to be excited within them, denoted as (13,13). The optimized structures of **1**, **5**, **7,** and **8** are given in Figure 1. The relative energies for **1**, **5**,and **7** are collected in Table 2. We can see that the CASSCF(13,13)/6-311G(2df) structures are in good agreement with the B3LYP and QCISD/6-311G(d) results. Also, the CASPT2(13,13)/6-311G(2df) //CASSCF(13,13)/6-311G(2df) relative energies are close to the CCSD(T)/6-311G(2d)//B3LYP/6-311G(d) and QCISD/6-311G(d) values. For the cyclic systems such as isomers **7** and **8**, the CASSCF results show that leading electronic configuration of **7** is 12-$(a1)^2 3(b1)^2 5(b2)^2 b1^1$, with contribution of 87.5%, while that of **8** is $14(a')^2 6(a'')^2 a'^1$ with contribution of 81.0%. These leading configurations are the electronic configuration spanned the Slater Determinant of B3LYP. This indicates that the multireference effect may be minor for the present system. It should be noted that inclusion of the *f*-function is important in calculating the relative energy of isomer **5**.

4. Conclusions

In conclusion, the lowest-energy isomer is found to be linear SiCCP **1**. Two cyclic species, i.e., cSiCCP **5** with Si−C cross bonding and cSiCPC **7** with C−C cross bonding, are energetically very close to **1** at just 3.2 and 10.4 kcal/mol, respectively, at the CCSD(T)/6-311+G(2df)//QCISD/6-311G(d)+ZPVE level. Moreover, each isomer contains considerable kinetic stability toward isomerization and dissociation. They might be observable in the laboratory and in interstellar space. On the other hand, the two cyclic forms **5** and **7** may be of particular interest since very few Si-containing cyclic species ($cSiC_2$, $cSiC_3$, and cSi_2C_2) have been detected in the laboratory or in interstellar space. No cyclic species containing both Si and P are known up to now, either. Therefore, we expect that species **5** and **7** may represent two new promising cyclic candidates to be detected in future. The results are also expected to be useful for understanding the initial growing step for the P-doped SiC vaporization processes.

Acknowledgment. This work is supported by the National Natural Science Foundation of China (Nos. 29892168, 20073014, 20103003, 20173021), Doctor Foundation of Educational Ministry, Foundation for University Key Teacher by the Ministry of Education and Key Term of Science and Technology by the Ministry of Education of China Foundation of Science and Technology Development for Jinlin Province of China. The authors are greatly thankful to the reviewers' invaluable comments.

Supporting Information Available: Table S-1 shows the harmonic vibrational frequencies and corresponding infrared intensities of interconversion transition states between SiC_2P isomers at the B3LYP/6-311G(d) level. This material is available free of charge via the Internet at http://pubs.acs.org.

References and Notes

(1) (a) Winnewisser, G. *J. Mol. Struct.* **1997**, *408/409*, 1. (b) McCarthy, M. C.; Apponi, A. J.; Thaddeus, P. *J. Chem. Phys.* **1999**, *110*, 10645. (c) Apponi, A. J.; McCarthy, M. C.; Gottlieb, C. A.; Thaddeus, P. *J. Chem. Phys.* **1999**, *111*, 3911.

(2) Michalopoulos. D. L.; Geusic, M. E.; Langriddge-Smith, P. R. R.; Smalley, R. E. *J. Chem. Phys.* **1984**, *80*, 3552.

(3) Grev, R. S.; Schaefer. H. F. *J. Chem. Phys.* **1984**, *80*, 3552.

(4) Alberts, I. L.; Grev, R. S.; Schaefer, H. F. *J. Chem. Phys.* **1990**, *93*, 5046.

(5) (a) Guélin, M.; Thaddeus, P. *Astrophys. J.* **1977**, *212*, L81. (b) McCarthy, M. C.; Gottlieb, C. A., Thaddeus, P.; Hom, M.; Botschwina, P. *J. Chem. Phys.* **1995**, *103*, 7820, and references therein. (c) Francisco, J. S. *Chem. Phys. Lett.* **2000**, *324*, 307, and references therein.

(6) del Rio, E.; Barrientos, C.; Largo, A. *J. Phys. Chem.* **1996**, *100*, 585−593.

(7) Ding, Y. H.; Li, Z. S.; Huang, X. R.; Sun, C. C. *J. Phys. Chem. A* **2001**, *105* (24), 5896−5901.

(8) Lammertsma, K.; Gûner, O. F. *J. Am. Chem. Soc*. **1988**, *110*, 5239. (b) Trucks, G. W.; Bartlett, R. J. *J. Mol. Struct*. (THEOCHEM) **1986**, *135*, 423.

(9) Furthmller, J.; Bechstedt, F.; Hsken, H.; Schrter, B.; Richter, W. *Phys. Rev. B* **1998**, *58*, *13712*, L1.

(10) Armitage, D. A. In *The Silicon-heteroatom Bond*; Patai, S., Rappoport, Z., Eds.; J. Wiley: New York, 1989; p151. Ibid., 1991; p183.

(11) (a) Frisch, M. J.; Trucks, G. W.; Schlegel, H. B.; Scuseria, G. E.; Robb, M. A.; Cheeseman, J. R.; Zakrzewski, V. G.; Montgomery, J. A., Jr.; Stratmann, R. E.; Burant, J. C.; Dapprich,S.; Millam, J. M.; Daniels, A. D.; Kudin, K. N.; Strain, M. C.; Farkas, O.; Tomasi, J.; Barone, V.; Cossi, M.; Cammi, R.; Mennucci, B.; Pomelli, C.; Adamo, C.; Clifford, S.; Ochterski, J.; Petersson, G. A.; Ayala, P. Y.;Cui, Q.; Morokuma, K.; Malick, D. K.; Rabuck, A. D.; Raghavachari, K.; Foresman, J. B.; Cioslowski, J.; Ortiz, J. V.; Stefanov, B. B.; Liu, G.; Liashenko, A.; Piskorz, P.; Komaromi, I.; Gomperts, R.; Martin, R. L.; Fox, D. J.; Keith, T.; Al-Laham, M. A.; Peng, C. Y.; Nanayakkara, A.; Gonzalez, C.; Challacombe, M.; Gill, P. M. W.; Johnson, B.; Chen, W.; Wong, M. W.; Andres, J. L.; Gonzalez, C.; Head-Gordon, M.; Replogle, E. S.; Pople, J. A. *Gaussian 98*, Revision A.6; Gaussian, Inc.: Pittsburgh, PA, 1998. (b) Andersson, K.; Barysz, M.; Bernhardsson, A.; Blomberg, M. R. A.; Carissan, Y.; Cooper, D. L.; Cossi, M.; Fleig, T.; Fülscher, M. P.; Gagliardi, L.; de Graaf, C.; Hess, B. A.; Karlström, G.; Lindh, R.; Malmqvist, P.-Å.; Neogrády, P.; Olsen, J.; Roos, B. O.; Schimmelpfennig, B.; Schütz, M.: Seijo, L.; Serrano-Andrés, L.; Siegbahn, P. E. M.; Stålring, J.; Thorsteinsson, T.; Veryazov, V.; Wierzbowska, M.; Widmark, P.-O. *MOLCAS*, Version 5.2; Lund University, Sweden 2001.